



# Mutational Analysis of the Mitochondrial DNA Displacement-Loop Region in Human Retinoblastoma with Patient Outcome

Lata Singh<sup>1</sup> · Neeru Saini<sup>2</sup> · Neelam Pushker<sup>3</sup> · Sameer Bakhshi<sup>4</sup> · Seema Sen<sup>1</sup> · Tapas C. Nag<sup>5</sup> · Seema Kashyap<sup>1</sup>

Received: 5 June 2017 / Accepted: 21 February 2018 / Published online: 12 March 2018  
© Arányi Lajos Foundation 2018

## Abstract

Alteration in mitochondrial DNA plays an important role in the development and progression of cancer. The Displacement Loop (D-loop) region of mitochondrial DNA (mtDNA) is the regulatory region for its replication and transcription. Therefore, we aimed to characterize mutations in the D-loop region of mitochondrial DNA along with the morphological changes and analyzed their impact on survival in retinoblastoma patients. mtDNA D-loop region was amplified by Nested-Polymerase Chain Reaction (Nested-PCR) and mutations were analyzed in 60 tumor samples from retinoblastoma patients by DNA sequencing. Transmission electron microscopy was performed on 5 retinoblastoma specimens. Mutations were correlated with clinical, histopathological parameters and patient survival. D-loop mutations were found in total of 52/60 (86.6%) patients. The most common mutations were T to C and C to T followed by A to G. There were 5.81% mutations which were not previously reported in the MITOMAP database. A73G (83.33%) were the most frequent mutations found in our cases and it was statistically significant with poor tumor differentiation and age. In addition, this study was further analyzed for morphological changes in retinoblastoma that had disorganized, swollen and less numbers of mitochondria on electron microscopy. This is the first study showing high frequency of mtDNA mutation which might be due to abnormal morphology of mitochondria in retinoblastoma. Our results indicate that pathogenic mtDNA D-loop mutations may be involved in tumorigenesis of retinoblastoma tumor.

**Keywords** Retinoblastoma · D-loop · Mitochondrial DNA · DNA sequencing · Electron microscopy

## Introduction

Mammalian cells possess nuclear and mitochondrial genome which comprises a dual genetic system. [1] The mitochondrion is a key venue for regulation of cell metabolism and

consider as the powerhouse of the cell. [2] It has also shown to play an important role in reactive oxygen species (ROS) generation, cell signaling, apoptosis, and metabolic pathways, including the Krebs cycle,  $\beta$ -oxidation, and lipid and cholesterol synthesis. [3] Mitochondrial DNA (mtDNA) contains 16,569 base pair genome in 100-1000 copies per cell contains 37 genes encoding 13 genes for respiratory chain subunits, 22tRNA and 2 ribosomal RNAs essential for protein synthesis. [4] The mitochondrial genome is more susceptible to oxidative damage and prone to higher rate of mutation than the nuclear genome [5]. The mutation frequency in mtDNA is about 10- to 20-fold greater in comparison to nuclear DNA due to lack of protective histone proteins and DNA repair mechanism [6].

D-loop (1124bp) region is the only non-coding segment of mtDNA containing regulatory elements that are involved in its replication and thus mutations in the D-loop may affect its copy number. This region considered to be a mutational hot spot region in various human cancers [7]. There are two hyper variable (HV) sites known as HVR-I considered as “low

---

Lata Singh and Seema Kashyap contributed equally to this work.

✉ Lata Singh  
lata.aiims@gmail.com

✉ Seema Kashyap  
dr\_skashyap@hotmail.com

<sup>1</sup> Department of Ocular Pathology, Dr. R. P. Centre for Ophthalmic Sciences, All India Institute of Medical Sciences, New Delhi, India

<sup>2</sup> Functional Genomics Unit, Institute of Genomics and Integrative Biology, Mall Road, New Delhi, India

<sup>3</sup> Department of Ophthalmology, Dr. R. P. Centre for Ophthalmic Sciences, All India Institute of Medical Sciences, New Delhi, India

<sup>4</sup> Department of Medical Oncology, IRCH, All India Institute of Medical Sciences, New Delhi, India

<sup>5</sup> Department of Anatomy, All India Institute of Medical Sciences, New Delhi, India

resolution” region (np16024–np16383) and HVR-II considered as “high resolution” region (np57–np372). This region regulates transcription and replication of mitochondrial DNA [8].

Genomic instability in the mtDNA region may be involved in tumorigenesis [9]. Mitochondria and their relations to the cancer have generated lot of interest these days in ongoing research. Advances in light microscopy and electron microscopy for assessment of cell components are fundamental for the better understanding of their relationships in health and disease [10]. Morphological changes of mitochondria in cancer are associated with mitochondrial-DNA mutations, tumor-microenvironment conditions and changes in mitochondrial oxidative phosphorylation (OXPHOS) complexes [11]. Contributions of mtDNA mutations have been recently proposed in the mitochondrial genome for the development of cancer cells.

The occurrence and progression of retinoblastoma is due to RB1 gene mutation and various other factors [12]. Although focus of research is on oncogenes and tumor suppressor genes, a lot of unanswered questions for metabolic alterations cannot be explained till now. Recent studies focused on understanding the various ophthalmologic manifestations and their implications into the pathogenesis and emerging therapies for mitochondrial-related ophthalmologic disorders. Till date, there are no studies in literature which have correlated mitochondrial mutations with patient outcome in retinoblastoma.

The aim of this study was to evaluate the frequency of mutations in D-loop region of mtDNA in human retinoblastoma tumor and correlated with clinicopathological factors, tumor differentiation and patient outcome. In addition to this, we performed transmission electron microscopy (TEM) for morphological changes.

## Material & Methods

### Sample Collection

Fresh tumor tissues of 60 primary enucleated retinoblastoma specimens and normal retina from non-neoplastic intraocular lesion were collected in the Department of Ocular Pathology, All India Institute of Medical Sciences, New Delhi, India and frozen at  $-70^{\circ}\text{C}$ . At the time of grossing,  $1\text{ m} \times 1\text{ mm}$  of tissue was kept in glutaraldehyde (fixative reagent) for electron microscopy. None of them had received prior radiation therapy or chemotherapy. Informed consent from all patients in this study was obtained under protocols approved by the institute ethics committee, AIIMS, New Delhi, India.

### Clinical Details

The tissue samples were processed and stained with hematoxylin and eosin (H&E) stain, and then analyzed under the microscope. The clinical and histopathological data of all patients were recorded. Hematoxylin and eosin (H & E) stained sections were reviewed for histopathological parameters like necrosis, calcification and histopathological high risk parameters, including retrolaminar optic nerve invasion, resected margin of optic nerve, massive choroidal, scleral, anterior chamber, iris and ciliary body involvement. Tumour differentiation was histologically classified into poorly differentiated Rb (<50% of Flexner– Wintersteiner rosettes) and well-differentiated Rb (>50% of Flexner– Wintersteiner rosettes). The pathological TNM staging was done according to the guidelines of the American Joint Committee on Cancer classification system.

### Nested-Polymerase Chain Reaction of D-Loop

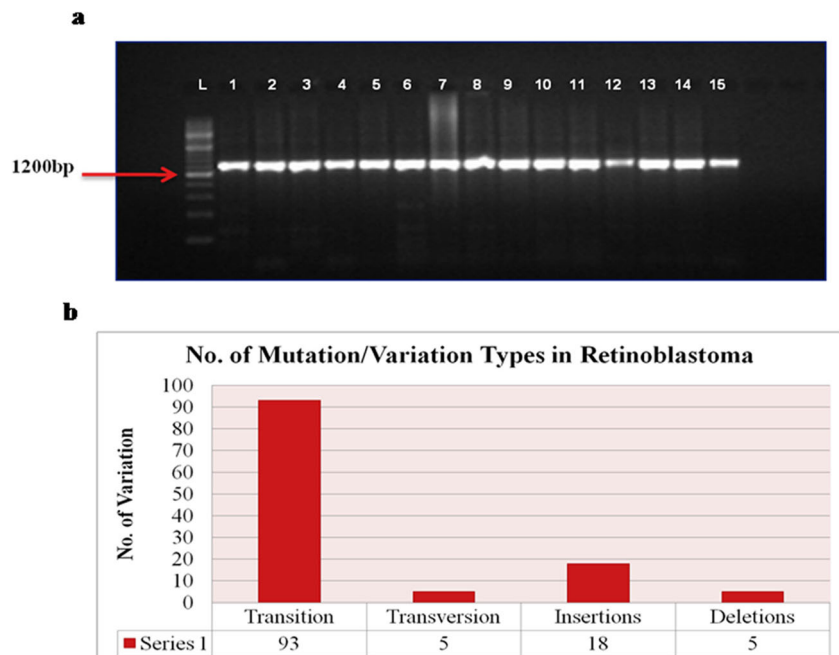
DNA was isolated from tissue using DNeasy blood and tissue kit (Qiagen, Dusseldorf, Germany) as per the manual. Nested-Polymerase Chain Reaction (PCR) was performed to amplify mitochondrial D-loop region. Outer primers were used to amplify the whole D-loop region (Product Size: 1298 bp) using the forward primer OUTER F1 (5'-GCCCATACCCCGAA AATGTTG- 3') and reverse primer OUTER R1 (5'-GGTAGAACTGCTATTATTCATCC-3'). For evaluation of internal fragment of D-loop region for two PCR products at 855 bp and 674 bp, were amplified from within the 1298 bp product using overlapping primers D1F 5'CTGTTCTTTCATGGGAAGC3' and D1R 5'GCTGTGCAGACATTCAATTGTT3'; D2F 5'GAGCTCTCCATGCATTTGGT3' and D2R 5'GGGGATGCTTGCATGTGTA3'. A total of 500ng of genomic DNA was used for nested PCR. PCR Conditions for amplification for the whole D-loop region were as follow: initial denaturation at  $94^{\circ}\text{C}$  for 3 min; 35 cycles of denaturation at  $94^{\circ}\text{C}$  for 45s; annealing at  $58^{\circ}\text{C}$  for 1 min; elongation at  $74^{\circ}\text{C}$  for 30s. PCR conditions for internal fragments of the D-loop were as follows: initial denaturation at  $94^{\circ}\text{C}$  for 3 min; 35 cycles of denaturation at  $94^{\circ}\text{C}$  for 30 s; annealing at  $56^{\circ}\text{C}$  for 30 s; elongation at  $72^{\circ}\text{C}$  for 45 s with a final extension at  $72^{\circ}\text{C}$  for 8 min (ABI Thermal Cycler). PCR products were purified using a GeneJet gel extraction kit (Thermo Fisher Scientific) and separated on 2.0% agarose gel. Normal retina was taken from non-neoplastic intraocular lesions as a control sample.

### DNA Purification and DNA Sequencing

After PCR amplification, samples were run in 0.8% agarose gel and purified using GeneJET Gel Extraction Kit (Thermo Scientific, K0691 and K0692). The gel slice containing the

DNA fragment was excised using a clean scalpel or razor blade. The gel slice was placed into a pre-weighed 1.5ml tube and weight was recorded. 100µl of binding buffer was added for every 100mg of agarose gel. The gel mixture was incubated at 50-60°C for 10 min. After solubilization, upto 800µl of the solubilized gel solution was transferred to the GeneJET purification column and centrifuged for 1 min. The flow through was discarded and column was placed back into the same collection tube. 100µl of binding buffer was added to GeneJET purification column and centrifuged for 1 min. The flow through was discarded and column was placed back into the same collection tube. 700µl of wash buffer was added to the GeneJET purification column and centrifuged for 1 min. The flow through was discarded and column was placed back into the same collection tube. The empty GeneJET purification column for an additional 1 min was centrifuged to completely remove residual wash buffer. The GeneJET purification column was then transferred into a clean 1.5ml microcentrifuge tube. Finally, 50µl of elution buffer was added to the center of the purification column membrane and centrifuged for 1 min. The purified DNA was stored at -20°C and DNA sequencing was performed (ABI 3730 XL; Applied Biosystems Instruments, Foster City, CA, USA). DNA sequencing was possible for up to 850–1000 bp in one reaction; as the D-loop (1120 bp) was sequenced in two overlapping fragments; the entire region of the D-loop was sequenced. PCR products were sequenced from both the directions to ensure reading accuracy. Sequences and chromatograms obtained from tumor samples and normal control were examined by latest version of Revised Cambridge Reference Sequence (rCRS) of human mitochondrial DNA and simultaneously analyzed for variation in sequences by Mito Tool programming. (<http://www.mitomap.org/bin/view/MITOMAP>).

**Fig. 1 a** Mitochondrial D-loop (mtD-loop) PCR (L = Ladder; 1–14: Tumor Samples; 15 = Control). **b** Types of Mutations found in Retinoblastoma



## Transmission Electron Microscopy (TEM)

Small pieces (1mm x 1mm) of 5 retinoblastoma tumor tissues were taken from enucleated specimens. Tissue samples were fixed in 2.5% glutaraldehyde and 2% paraformaldehyde in 0.1 M sodium phosphate buffer (pH 7.3) for 12 hours at 40 C. The samples were post fixed in 1% OsO<sub>4</sub> for 1 hour at 40 C after washing with buffer. The samples were dehydrated in acetone, infiltrated and embedded in araldite CY 212 (TAAB, UK). Thick Sections (1 µm) were cut with an ultramicrotome. These sections were then mounted on to glass slides, stained with aqueous toluidine blue and observed under a light microscope for gross observation of the area and quality of the tissue fixation. Thin sections of grey-silver color interference (70-80 nm) were cut and mounted onto 300 mesh-copper grids for electron microscopic examination. Sections were stained with alcoholic uranyl acetate and alkaline lead citrate, washed gently with distilled water. Then, sections were observed under a Morgagni 268D transmission electron microscope (Fei Company, The Netherlands) at an operating voltage 80 kV. Images of sections were digitally acquired by CCD camera (Megaview III, Fei Company) using iTEM software (Soft Imaging System, Münster, Germany) attached to the microscope.

## Statistical Analysis

Mitochondrial D-loop mutations were correlated with clinical and histopathological parameters using the chi-square test. *p* value <0.05 was considered statistically significant. D-loop mutations correlated with overall survival of patients by Kaplan Meier Analysis. We considered only those mutations which were present in four or more patients.

**Table 1** Most frequent mutations in different positions of d-loop region

S.No.	Position	Mutation	Change	No. of Patients
1.	56	Transition	A: T	1
2.	60	Deletion	T: DEL	2
3.	71	Insertion	G: GG	1
4.	<b>73</b>	<b>Transition</b>	<b>A: G</b>	<b>9</b>
5.	93	Insertion	A: AA	1
6.	107	Insertion	G: GG	1
7.	152	Transition	T: C	1
8.	155	Insertion	T: TT	3
9.	171	Insertion	G: GG	1
10.	183	Transition	A: G	1
11.	185	Insertion	G: GG	1
12.	195	Transition	T: C	1
13.	211	Transition	A: G	1
14.	240	Transition	A: G	2
15.	252	Transition	T: C	1
16.	<b>263</b>	<b>Transition</b>	<b>A: G</b>	<b>19</b>
17.	309	Insertion	C: CCCT	7
18.	310	Transition	T: C	1
19.	319	Transition	C: T	3
20.	323	Transversion	C: G	1
21.	411	Transversion	C: G	1
22.	461	Transition	C: T	1
23.	482	Transition	T: C	1
24.	511	Transition	C: T	1
25.	563	Transition	A: G	1
26.	16050	Insertion	T: TT	1
27.	16092	Deletion	T: DEL	1
28.	16126	Transition	T: C	2
29.	16150	Transition	C: T	1
30.	16151	Transition	C: T	1
31.	16163	Transition	A: G	1
32.	16180	Deletion	A: DEL	1
33.	16186	Transition	C: T	2
34.	16189	Transition	T: C	1
35.	16207	Transition	A: G	1
36.	16215	Deletion	T: DEL	1
37.	16220	Deletion	A: DEL	1
38.	16222	Deletion	C: DEL	1
39.	<b>16223</b>	<b>Transition</b>	<b>C: T</b>	<b>12</b>
40.	16225	Transition	C: T	1
41.	16228	Transition	C: T	1
42.	16234	Transition	C: T	1
43.	16239	Transition	C: T	1
44.	16254	Transition	A: G	1
45.	16256	Transition	C: T	1
46.	16270	Transition	C: T	1
47.	16294	Transition	C: T	1
48.	16311	Transition	T: C	1
49.	16333	Transversion	A: T	2
50.	16391	Insertion	G: GG	1
51.	<b>16519</b>	<b>Transition</b>	<b>T: C</b>	<b>15</b>
52.	16536	Transversion	C: A	1
53.	16542	Transition	C: T	1
54.	16549	Insertion	C: CC	1
55.	16561	Transition	A: T	1

Bold specifies most frequent mutations in our cases

## Results

### Clinicopathological Details

The mean age of the 60 primary enucleated Rb cases was 2.8 years. The most common presenting symptoms were

leukocoria followed by decreased vision and strabismus. There was a male preponderance (58%) and 21.7% cases were bilateral in our study. Higher pTNM staging (T3 + T4) was found in 32 (53.3%) cases. The tumour was poorly differentiated in 45/60 (75%) with necrosis and calcification in 61.66% and 28.33% cases respectively. Massive choroidal invasion was observed in 20 cases and histopathological high risk factors in 33.3% cases. Tumour invasion/HRFs were identified in 25/60 (41.7%) cases. Follow-up data were obtained in all patients for a period of 6–30 months.

### DNA Sequencing

Mitochondrial D-loop PCR was performed in all the cases to analyze mutation in D-loop region (Fig. 1a). The mtDNA D-loop was sequenced from 60 retinoblastoma cases to assess the presence of somatic mutations with respect to the inherited mtDNA sequence. The Cambridge sequence of the mtDNA D-loop was used as a reference (MITOMAP). D-loop mutation were found in total of 52/60 (86.6%) patients when compared to normal retinal tissue. We found 121 mutation on 55 positions and 8 novel mutations on comparing with the rCRS (MITOMAP) database in our study (Tables 1 and 2). The frequency of mutations at 16519 T to C (28.8%), 16223C to T (23.1%), 263A to G (36.5%) and 73A to G (17.3%) were significantly higher in our study. All mutations were single nucleotide substitutions (Fig. 1b). Majority of these somatic mutations of mtDNA were homoplasmic as compared to heteroplasmic. The most common mutations were T to C and C to T followed by A to G (Fig. 2). Most of the mutations were found in hypervariable regions (HVI and HVII). The common instabilities were observed at the first polymorphic C track (np303–315, named D310). Haplogroup T1a (T1a1'3) was commonly found in retinoblastoma cases as it had HSV1 transition on 16126, 195 & 16294 positions. These Haplogroup was found mostly in India, England, Algeria and Greece.

(Source of information: [http://www.eupedia.com/europe/Haplogroup\\_T\\_mtDNA.shtml](http://www.eupedia.com/europe/Haplogroup_T_mtDNA.shtml))

**Table 2** Novel mutations found in retinoblastoma cases

S.No.	Position No.	Mutation
1.	71	G: GG
2.	107	G: GG
3.	155	T: TT
4.	185	G: GG
5.	291	A: AA
6.	593	T: TG
7.	16050	T: TT
8.	16339	C: A

**Fig. 2** D-loop mutations at most frequent positions in retinoblastoma cases on mitomap analysis

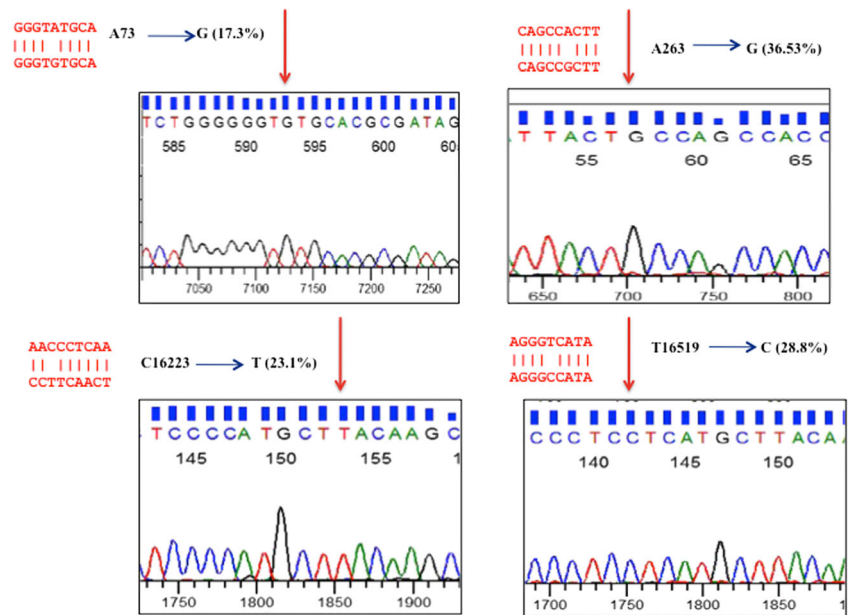


**Table 3** Correlation of 16,519 T to C and 16223C to T mutation with clinicopathological parameters

Pathological	16,519 T to C Mutation			16223C to T Mutation		
	Negative (n = 37)	Positive (n = 15)	p-value	Negative (n = 40)	Positive (n = 12)	p-value*
Parameters N: 52						
Sex						
Female (25)	18	7	0.893	15	10	<b>0.012</b>
Male (27)	19	8		25	2	
Age						
< 2 years (21)	15	6	0.971	15	6	0.441
> 2 years (13)	12	9		25	6	
Laterality						
Bilateral (40)	28	12	0.738	33	7	0.091
Unilateral (12)	9	3		7	5	
Staging						
T3+ T4 (29)	18	11	0.112	20	9	0.137
T1 + T2 (23)	19	4		20	3	
Differentiation						
PDRB (37)	28	9	0.263	32	5	<b>0.015</b>
WDRB (15)	9	6		8	7	
Necrosis						
No (19)	14	5	0.760	14	5	0.675
Yes (33)	23	10		26	7	
Calcification						
No (37)	28	9	0.263	28	9	0.738
Yes (15)	9	6		12	3	
Choroidal Invasion						
Massive (35)	23	12	0.222	26	9	0.579
Focal (17)	14	3		14	3	
AC Invasion						
No (48)	35	13	0.346	37	11	0.924
Yes (4)	2	2		3	1	
Scleral Invasion						
No(45)	31	14	0.376	34	11	0.559
Yes(7)	6	1		6	1	
Iris/CB Invasion						
No (46)	33	13	0.797	36	10	0.530
Yes (6)	4	2		4	2	
ON (Head)						
No (39)	28	11	0.860	31	8	0.450
Yes (13)	9	4		9	4	
ON Invasion (RL & CE)						
No (38)	27	11	0.979	26	12	1.000
Yes (14)	10	4		14	0	
Tumor Invasion						
No (29)	18	11	0.978	20	9	0.137
Yes (23)	19	4		20	3	

Bold represent statistically significant values by Fisher's Exact Test

## TEM Results

Tumor samples of retinoblastoma specimens were examined by means of TEM. All cases showed high nucleocytoplasmic ratio. Mitochondria exhibited a heterogeneous morphology in each of the cases (Figure 4a and b). Swollen mitochondria

with partial or complete cristolysis were the most commonly altered feature observed in retinoblastoma cases compared to normal retina along with different form of mitochondria like giant, elongated (Figure c and d). All these cases showed mutations which were found at most frequent sites in sequencing.

**Table 4** Correlation of 263 A to G and 73A to G mutation with clinicopathological parameters

Pathological	263 A to G Mutation		p-value*	73A to G Mutation		p-value*
	Negative ( <i>n</i> = 33)	Positive ( <i>n</i> = 19)		Negative ( <i>n</i> = 43)	Positive ( <i>n</i> = 9)	
Parameters						
N: 52						
Sex						
Female (25)	17	8	0.514	20	5	0.514
Male (27)	16	11		23	4	
Age						
< 2 years (21)	8	13	<b>0.003</b>	16	5	<b>0.003</b>
> 2 years (13)	25	6		27	4	
Laterality						
Bilateral (40)	28	12	0.082	33	7	0.947
Unilateral (12)	5	7		10	2	
Staging						
T3+ T4 (29)	16	13	0.167	24	5	0.989
T1 + T2 (23)	17	6		19	4	
Differentiation						
PDRB (37)	29	8	<b>0.001</b>	31	6	0.744
WDRB(15)	4	11		12	3	
Necrosis						
No (19)	10	9	0.222	14	5	0.202
Yes (33)	23	10		29	4	
Calcification						
No (37)	25	12	0.337	29	8	0.223
Yes (15)	8	7		14	1	
Choroidal Invasion						
Massive (35)	20	15	0.181	29	6	0.964
Focal (17)	13	4		14	3	
AC Invasion						
No (48)	30	18	0.622	39	9	1.000
Yes (4)	3	1		4	0	
Scleral Invasion						
No (45)	27	18	0.217	37	8	0.821
Yes (7)	6	1		6	1	
Iris/CB Invasion						
No (46)	29	17	0.862	38	8	0.965
Yes (6)	4	2		5	1	
ON (Head)						
No (39)	24	15	0.619	32	7	0.833
Yes (13)	9	4		11	2	
ON Invasion (RL & CE)						
No (38)	23	15	0.471	31	7	0.727
Yes (14)	10	4		12	2	
Tumor Invasion						
No (29)	16	13	0.167	24	5	0.989
Yes (23)	17	6		19	4	

Bold represent statistically significant values by Fisher's Exact Test

## Statistical Analysis

The association of mitochondrial D-loop mutations with clinicopathological parameters and patient outcome was analyzed using Fisher's exact test (as shown in Tables 3 and 4). Kaplan Meier survival analysis was carried out to determine the prognostic potential of D-loop mutation at frequent positions in retinoblastoma cases (Fig. 3a-d). There was no significant difference between the survival of patients with or without any mutations. Also no significant correlation was found between D-loop region and 16,519, 263 and 73rd positions (Table 5). Overall survival was less in retinoblastoma patients who showed presence of 16223C to T mutations which was statistically significant by Kaplan–Meier analysis ( $p$ -value = 0.0481).

## Discussion

The human mtDNA sequence is highly variable [13]. Functionally important mutations are essential to define the

pathogenesis and tumor progression in cancers. Human mtDNA has no introns but proportions of contiguous coding sequences are extremely high [14]. Mitochondria represent the major source of energy supply in ocular functions [15]. mtDNA genomic mutations are the major defect in the etiology of various ocular diseases.

Mutations in D-loop region have been reported in human cancers and various ophthalmic diseases [16]. There is increasing evidence to support an association between mitochondrial dysfunction and a number of ocular related pathologies involving Leber's hereditary Optic Neuropathy (LHON), [17] age-related macular degeneration (AMD), [18] diabetic retinopathy, [19] uveitis [20] and glaucoma. [21] Wallace DC et al [13] described LHON as the first maternally inherited ophthalmologic disorder which was linked to point mutation in mitochondrial complex I. Abu-Amro KK et al found G11778A mutation downregulates OPA1 expression using genome wide expression profiling in LHON patients leukocytes. Similarly, Mutation in mtDNA maintenance gene TYMP, ANT1, PEO1, POLG,

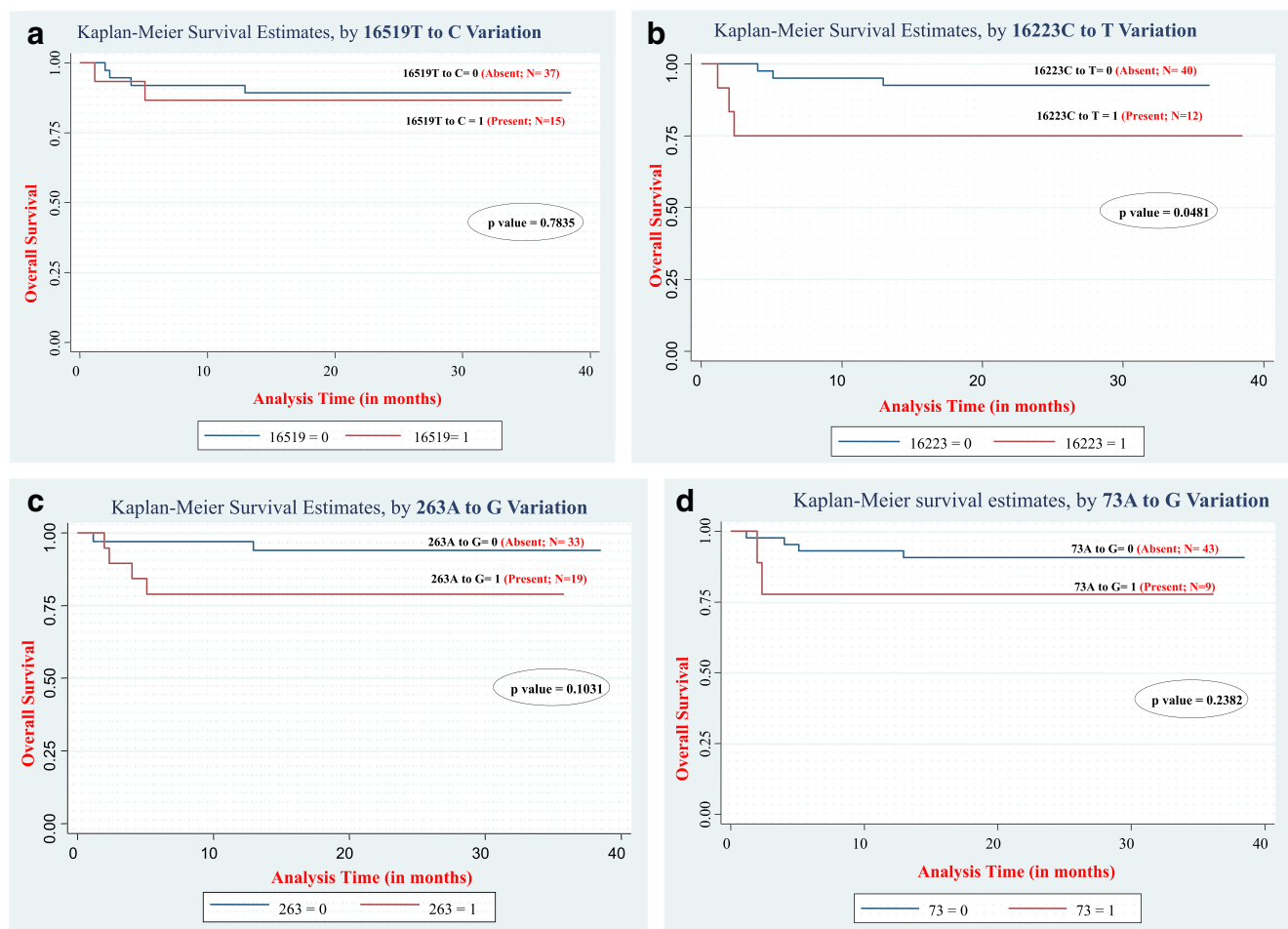


**Fig. 3** Kaplan Meier Curve showing Overall Survival Rate of Retinoblastoma Patients based on mutations at Frequent Sites. **a:** Overall survival rate of patients based on T16519C Mutation **b:** overall

survival rate of patients based on C16223T mutation **c:** Overall Survival rate of patients based on A263G MUTATION **d:** Overall survival rate of patients based on A73G mutation

**Table 5** Correlation of Overall Survival (OS) with pathological parameters and D-loop mutations estimated by Kaplan Meier survival analysis and comparison using log rank test

Parameters	OS	SE	CI	p-value*
Differentiation				
PDRB (37)	86.49%	0.0562	0.7–0.9	0.4966
WDRB (15)	93.33%	0.0644	0.6–0.9	
Necrosis				
No (19)	94.74%	0.0512	0.6–0.9	0.3011
Yes (33)	84.85%	0.0624	0.6–0.9	
Calcification				
No (37)	89.19%	0.0510	0.7–0.9	0.7835
Yes (15)	86.67%	0.0878	0.5–0.9	
Choroidal Invasion				
Massive (35)	88.57%	0.0538	0.7–0.9	0.9865
Focal (17)	88.24%	0.0781	0.6–0.9	
Scleral Invasion				
No (45)	88.89%	0.0468	0.7–0.9	0.7757
Yes (7)	85.71%	0.1323	0.3–0.9	
Anterior Chamber Invasion				
No (48)	87.50%	0.0477	0.7–0.9	0.4674
Yes (4)	100%	–	–	
Iris/Ciliary Body Invasion				
No (46)	89.13%	0.0459	0.7–0.9	0.6405
Yes (6)	83.33%	0.1521	0.2–0.9	
Optic Nerve (Head)				
No (39)	87.18%	0.0535	0.7–0.9	0.6283
Yes (13)	92.31%	0.0739	0.5–0.9	
ON Invasion (RL & Cut End)				
No (38)	89.47%	0.0498	0.7–0.9	0.6283
Yes (14)	85.71%	0.0935	0.5–0.9	
Tumor Invasion				
No (29)	89.66%	0.0566	0.7–0.9	0.7540
Yes (23)	86.96%	0.0702	0.6–0.9	
16519 T to C				
No (37)	89.19%	0.0510	0.7–0.9	0.7835
Yes (15)	86.67%	0.0878	0.5–0.9	
16223C to T				
No (40)	92.50%	0.0416	0.7–0.9	<b>0.0481</b>
Yes (12)	75.00%	0.1250	0.4–0.9	
263A to G				
No (33)	93.94%	0.0415	0.7–0.9	0.1031
Yes (19)	78.95%	0.0905	0.5–0.9	
73A to G				
No (43)	90.70%	0.0443	0.7–0.9	0.2382
Yes (9)	77.78%	0.1386	0.3–0.9	

Bold represent statistically significant values by Fisher's Exact Test

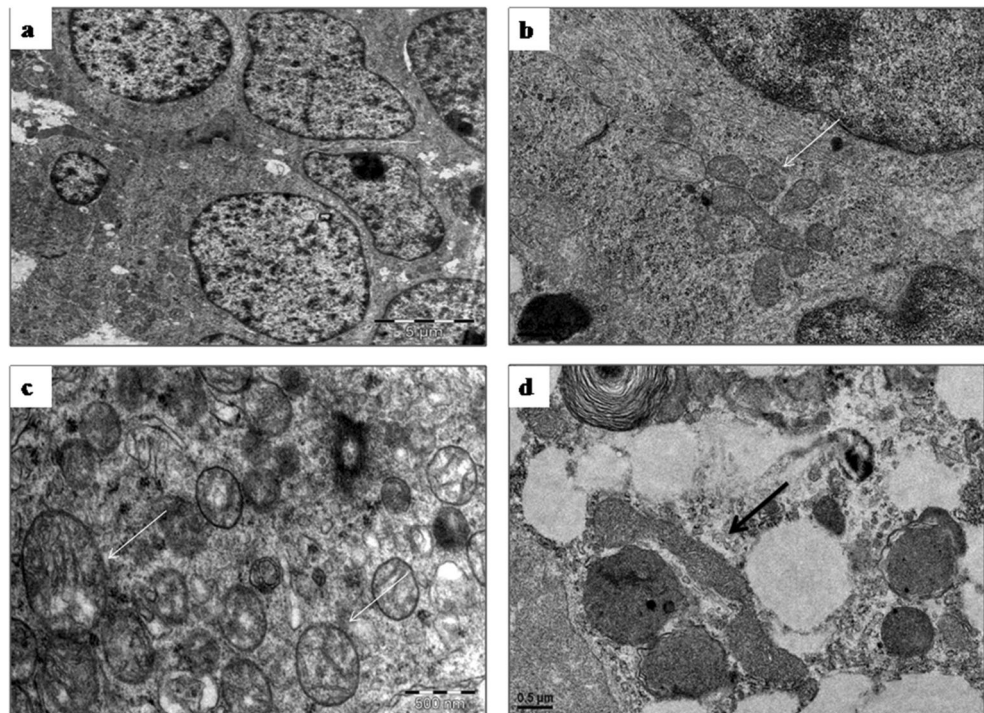
POLG2 and OPA1 were also found in chronic progressive external ophthalmoplegia (CPEO) [22].

Mutations in the mtDNA D-loop region and copy number changes were frequently found in colorectal and gastric malignancies, [14] lung cancer, [23] colon cancer, [24] ovarian cancer, [25] hepatocellular carcinoma, [26] breast cancer [27] and gastric cancer [28]. Therefore, mtDNA instability is a molecular hallmark used not only in forensic analyses, but also in medical diagnosis of cancer [29].

Among other tumor types studied, Miyazono et al. [30] analyzed the mutations of the mtDNA D-loop region and found mutations in 40% of the esophageal tumors, while another study revealed that D-loop mutations were much less frequent in esophageal tumors [31]. Fliss et al analyzed 50% of mtDNA mutations in bladder, head and neck, and lung cancer, of which 67% were in the mtDNA D-loop region. In ovarian cancers, 60% of somatic mutations in the D loop region along with 12s rRNA, 16s rRNA and cyt b have been reported [25]. Most of the mutations were T → C or G → A transitions. The only report on mtDNA mutations in cervical cancer has reported high frequency of D310 mutations in 35% of cases [32]. However, they have not looked at other mtDNA mutations besides D310.

We present comprehensive data of 60 retinoblastoma tissues and found that 86.6% samples showed mutation within D-loop region. Most of these mutations were single base substitution i.e. transition along with insertions or deletions. Our study also revealed mutation at D310

**Fig. 4 Ultrastructural Morphology of Mitochondria in Retinoblastoma Tumor Samples.** a & b showing heterogeneous morphology of tumor cell in retinoblastoma. c & d showing swollen and elongated form of mitochondria in tumor sample



site which is a poly C sequence present in 303–315 position of D-loop region in more than one sample. The majority of the base substitution mutations were transition (76.8%) in our study which is a characteristic feature of oxidative DNA damage. In the present study, there was a significant association of A263G mutation with poor differentiation ( $p=0.001$ ) and age ( $p=0.003$ ).

The present study shows that majority of detected mutations were homoplasmic. Changes in oxidative phosphorylation (OXPOS) system may be due to long term accumulation of homoplasmic mutations. Mitochondrial homoplasmic mutations have also been known to occur in cancerous lesions [33]. Our study found 16223 T to C mutation in 15/52 (28.8%) cases which was statistically significant with poor tumor differentiation and poor survival of the retinoblastoma patients. Mainly mutations at 16223 C to T and 16311 T to C are located at positions where Tfam (mitochondrial transcription factor) binds (16220–16325 bp) and regulates the transcriptome of mitochondria [34]. Changes in binding site or conformational change in mtDNA alters the binding capability of Tfam which in turn may modify the strength of mtDNA-protein complex. This may result in abnormal expression and development of mitochondrial genes and their cancer phenotypes [35].

To conclude, this is the first study that revealed high frequency of mitochondrial D-Loop mutations in patients with retinoblastoma tumor which supports the fact that that mitochondrial dysfunction is a factor in cancer etiopathogenesis, an insight that may suggest new approaches for diagnosis and treatment in retinoblastoma tumor. In future research, next generation sequencing might be used to identify novel genetic variants in whole mtDNA associated with retinoblastoma tumor in large cohorts of patients.

**Author Contribution** LS was responsible for designing and executing the experiment. NS helps in sequencing analysis. SK and SS did the histopathological evaluation. TCN did the electron microscopy evaluation. SB was responsible for providing follow up. NP was responsible proving samples.

**Funding** This study was funded by Indian Council of Medical Research, New Delhi, INDIA (Award no: 5/4/6/09/Oph/2012-NCD II).

## Compliance with Ethical Standards

**Conflict of Interest** No potential conflicts of interest with any author.

**Ethical Approval** All procedures performed in studies involving human participants were in accordance with the ethical standards of the institutional and/or national research committee and with the 1964 Helsinki declaration and its later amendments or comparable ethical standards.

**Informed Consent** Informed consent was obtained from all individual participants included in the study.

## References

- Larsson NG, Clayton DA (1995) Molecular genetics aspects of human mitochondrial disorders. *Annu Rev Genet* 29:151–178
- Lane N (2006) Mitochondrial disease: powerhouse of disease. *Nature* 440:600–602
- Falk MJ (2010) Neurodevelopmental manifestations of mitochondrial disease. *J Dev Behav Pediatr* 31:610
- Taanman JW (1999) The mitochondrial genome: structure, transcription, translation and replication. *Biochim Biophys Acta (BBA)-Bioenergetics* 9(1410):103–123
- Anderson S, Bankier AT, Barrell BG et al (1981) Sequence and organization of the human mitochondrial genome. *Nature* 290:457–465
- Vives-Bauza C, Gonzalo R, Manfredi G et al (2006) Enhanced ROS production and antioxidant defenses in cybrids harbouring mutations in mtDNA. *Neurosci Lett* 391:136–141
- Stoneking M (2000) Hypervariable sites in the mtDNA control region are mutational hotspots. *Am J Hum Genet* 67:1029–1032
- Van Oven M, Kayser M (2009) Updated comprehensive phylogenetic tree of global human mitochondrial DNA variation. *Hum Mutat* 30:E386–E394
- Mims MP, Hayes TG, Zheng S et al (2006) Mitochondrial DNA G10398A polymorphism and invasive breast cancer in African-American women. *Cancer Res* 66:1880–1881
- Janovjak H, Sapra KT, Kedrov A et al (2008) From valleys to ridges: exploring the dynamic energy landscape of single membrane proteins. *Chem Phys Chem* 9:954–966
- Arismendi-Morillo G (2011) Electron microscopy morphology of the mitochondrial network in gliomas and their vascular microenvironment. *Biochim Biophys Acta (BBA)-Bioenergetics* 1807:602–608
- Lohmann DR (1999) RB1 gene mutations in retinoblastoma. *Hum Mutat* 14:283–288
- Wallace DC, Chalkia D (2013) Mitochondrial DNA genetics and the heteroplasmy conundrum in evolution and disease. *Cold Spring Harb Perspect Biol* 5:a021220
- Alonso A, Martin P, Albarran C et al (1997) Detection of somatic mutations in the mitochondrial DNA control region of colorectal and gastric tumors by heteroduplex and single-strand conformation analysis. *Electrophoresis* 18:682–685
- Jarrett SG, Lewin AS, Boulton ME (2010) The importance of mitochondria in age-related and inherited eye disorders. *Ophthalmic Res* 44:179–190
- Schrier SA, Falk MJ (2011) Mitochondrial disorders and the eye. *Curr Opin Ophthalmol* 22:325–331
- Wallace DC, Singh G, Lott MT et al (1998) Mitochondrial DNA mutation associated with Leber's hereditary optic neuropathy. *Science* 242:1427
- Barreau E, Brossas JY, Courtois Y, Treton JA (1996) Accumulation of mitochondrial DNA deletions in human retina during aging. *Invest Ophthalmol Vis Sci* 37:384–391
- Kowluru RA (2005) Diabetic retinopathy: mitochondrial dysfunction and retinal capillary cell death. *Antioxid Redox Signal* 7:1581
- Saraswathy S, Rao NA (2009) Mitochondrial proteomics in experimental autoimmune uveitis oxidative stress. *Invest Ophthalmol Vis Sci* 50:5559–5566
- Tezel G (2006) Oxidative stress in glaucomatous neurodegeneration: mechanisms and consequences. *Prog Retin Eye Res* 25:490–513
- DiMauro S, Garone C (2010) Historical perspective on mitochondrial medicine. *Dev Disabil Res Rev* 16:106–113
- Suzuki M, Toyooka S, Miyajima K et al (2003) Alterations in the mitochondrial displacement loop in lung cancers. *Clin Cancer Res* 9:5636–5641

24. Habano W, Sugai T, Yoshida T et al (1999) Mitochondrial gene mutation, but not large-scale deletion, is a feature of colorectal carcinomas with mitochondrial microsatellite instability. *Int J Cancer* 2683:625–629
25. Liu VW, Shi HH, Cheung AN et al (2001) High incidence of somatic mitochondrial DNA mutations in human ovarian carcinomas. *Cancer Res* 61:5998–6001
26. Okochi O, Hibi K, Uemura T et al (2002) Detection of mitochondrial DNA alterations in the serum of hepatocellular carcinoma patients. *Clin Cancer Res* 8:2875–2878
27. Rosson D, Keshgegian AA (2004) Frequent mutations in the mitochondrial control region DNA in breast tissue. *Cancer Lett* 215:89–94
28. Tamura G, Nishizuka S, Maesawa C et al (1999) Mutations in mitochondrial control region DNA in gastric tumours of Japanese patients. *Eur J Cancer* 35:316–319
29. Levin BC, Cheng H, Reeder DJ (1999) A human mitochondrial DNA standard reference material for quality control in forensic identification, medical diagnosis, and mutation detection. *Genomics* 55:135–146
30. Miyazono F, Schneider PM, Metzger R et al (2002) Mutations in the mitochondrial DNA D-Loop region occurs frequently in adenocarcinoma in Barrett's esophagus. *Oncogene* 21:3780–3783
31. Hibi K, Nakayama H, Yamazaki T et al (2001) Mitochondrial DNA alteration in esophageal cancer. *Int J Cancer* 92:319–321
32. Sharma H, Singh A, Sharma C et al (2005) Mutations in the mitochondrial DNA D-loop region is frequent in cervical cancer. *Cancer Cell Int* 16:34
33. Chatterjee A, Mambo E, Sidransky D (2006) Mitochondrial DNA mutations in human cancer. *Oncogene* 25:4663–4674
34. Sharawat SK, Bakhshi R, Vishnubhatla S, Bakhshi S (2010) Mitochondrial D-loop variations in paediatric acute myeloid leukaemia: a potential prognostic marker. *Br J Haematol* 149:391–398
35. Richard SM, Bailliet G, Paez GL et al (2000) Nuclear and mitochondrial genome instability in human breast cancer. *Cancer Res* 60:4231–4237